MEASUREMENT OF THE SECONDARY ELECTRON-EMISSION COEFFICIENT FROM LOW-LOSS DIELECTRIC MATERIALS

Shingo Mori*[A)], Mitsuhiro Yoshida†[A)], Daisuke Satoh‡[B)]
[A)]KEK, Tsukuba, Japan
[B)]National Institute of Advanced Industrial Science and Technology, Tsukuba, Japan

Abstract

We are trying to measure the secondary electron emission coefficient of the ultra-low-loss dielectric cells used in the dielectric assist accelerating (DAA) structure. The DAA structure ideally is compatible with both high gradient and high efficiency, while the discharge from the corner of the dielectric cells near the beam axis and following multipactor limit the accelerating gradient. This problem would be defused by applying the TiN coating to the center region of the cells. We manufacture the device to measure the secondary electron coefficient of the cells, and trying to measure the effects of the coating by comparing the ones before and after the TiN coating. We will report the current status of the experiment.

INTRODUCTION

Radio-frequency (rf) linac structures with high efficiency and high gradient could play crucial roles not only in future investigation of the origin of the Higgs sector and the physics beyond the standard model in elementary particle physics, but also in industrial and medical applications such as material and radiation processing and cancer therapy, and the synchrotron radiation-based science. The highly efficient accelerators enable us to construct the accelerators capable of continuous operation at room temperature, which would provide a large number of statistics needed for the observation of the rare processes and the economic advantage for the industrial and the medical applications. The accelerators with high gradient allow us to construct both extremely high energy colliders, e.g. 100-TeV collider, and miniaturized linacs for the applications.

A dielectric assist accelerating (DAA) structure [1,2] appears to be very promising in terms of power efficiency. Figure 1 shows the conceptual structure of the multi-cell DAA cavity. It applies a standing wave of a higher order TM_{02n} mode for the accelerating mode, which consists of ultra-low loss dielectric cylinders and disks with irises which has periodicity in the beam direction. The dimensions of the dielectric structure are determined so that the peaks of the electric field is confined within the ceramics which has relatively high permittivity, $\epsilon_r \sim 10$ and can hold many electric force lines. In the radial direction, the coaxial dielectric layer partially confines the electromagnetic field in the cavity so that the surface magnetic field at the copper surface becomes relatively small compared to one of the pill-box cavity. It is known that the waveguides with dielectric disks have a higher shunt impedance than all-metal waveguides [3]. Naively, this is because the dielectric disks make the electric force line concentrated around the beam axis.

Due to the above efficient structures and the use of the ultra-low loss dielectric material [2], the five cell DAA cavity provides the Q-value, $Q = O(10^5)$, and the shunt impedance $Z_{sh} \simeq 650$ MΩ. The shunt impedance is defined as the ratio of the accelerating voltage V_{acc} and power loss in the cavity P_{loss}

$$Z_{sh} = \frac{V_{acc}^2}{2LP_{loss}}, \tag{1}$$

where L is the length of the cavity. Thus, the input power of 1 kW would produce the gradient of 1 MV/m. However, we found the input power is limited by a few kW which corresponds to the maximum gradient of multi-MV/m in the tentative high voltage test due to the breakdown caused by the multipactor at the surface of the dielectrics.

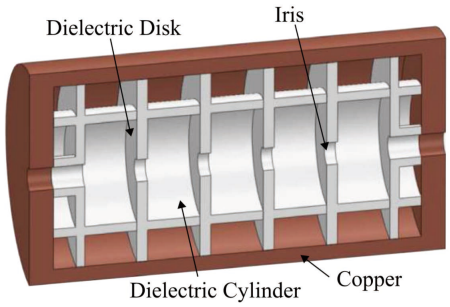

Figure 1: Conceptual illustration of a multi-cell DAA structure. This figure is taken from Ref. [2].

In rf applications, the multipactor effect [4] appear limiting the power of the electromagnetic waves. The mechanism of the multipactor is understood as an electron avalanche where the secondary electron emission (SEE) and the electrons from external sources couple with the alternating electric field. This process produces the electron cloud which losses the input power without increasing the gradient. The condition of the multipactor on dielectrics is studied in the literature [5,6] and the references therein.

The multipactor is naively understood by the energy dependence of the secondary electron emission coefficient (SEEC), $\delta(E_p)$, which is defined as the ratio of the number of emitted electrons in the number of injected electrons, where E_p is the electron impact energy on the dielectric surface. Naively, the multipactor could occur if $\delta(E_p) > 1$,

* smori@post.kek.jp
† mitsuhiro.yoshida@kek.jp
‡ dai-satou@aist.go.jp

where the typical impact energy is determined by the normal component of the electric field to the dielectric surface. The empirical formula [7] of the energy dependence of the SEEC is known as

$$\delta(E_p) \simeq \delta_{\max}(we^{1-w})^k, \tag{2}$$

where $w = E_p/E_{\max}$ and $E_{\max}$ is the primary electron energy which yields $\delta_{\max}$. $k = 0.62$ for $w < 1$ and $k = 0.25$ for $w > 1$. This formula tells us that the multipactor could happen in the limited gradient region, and in the larger gradient region corresponding to $\delta(E_p) < 1$ the cavity may be free from the breakdown. Thus, our issue to get higher gradient with DAA structure is how to avoid the multipactor effect.

The TiN coating can reduce the SEEC drastically and is the standard method in the manufacturing of the rf window. Since TiN coating could increase the power loss on its surface and spoil the benefit from the use of ultra low loss dielectrics. As a simple solution, we are trying to apply a TiN coating on the dielectrics in DAA structure only around the beam axis where a relatively strong electric field is applied and we found the traces of discharge after the high voltage test. In order to investigate the effectiveness of TiN coating on the ultra low loss dielectrics, we try to measure the SEEC in both dielectric cells before and after TiN coating. In this paper, we will report the current status of our experiment.

This paper is organized as follows. In Sec. Methods, the dielectric cell of the DAA structure is introduced and the experimental setup to measure the SEEC of the dielectrics is described. In Sec. Conclusion, we will summarize our current status of the experiment and discuss the future study of the DAA structure.

METHODS

The schematic picture of the experiment is shown in Fig. 2. As an electron source, we use the photoelectron emitted from the aluminum target. The primary electron energy E_p is tuned by the gap between the aluminum target and the outer cup, where we change the negative voltage of the aluminum target from −0.1 kV to −2.0 kV. The purple dashed line denotes the ultra-violet laser with wavelength 257 nm. The primary electrons shown as the green dashed line pass through the Faraday cup whose current is denoted as I_p, and hit the target put below the cup. The secondary electrons shown as red dashed line emitted from the target and captured by the inner cup which is biased by 50 V so that all secondary electrons could be captured. The current of the secondary electrons I_s is measured using a picoammeter. Note that the hole of the inner cup is much larger than one of the outer cup, so that the secondary current I_s contains purely the secondary electrons and does not include the primary electrons.

The SEEC δ is defined as the ratio of the number of the injected electrons and one of the ejected electrons. Thus,

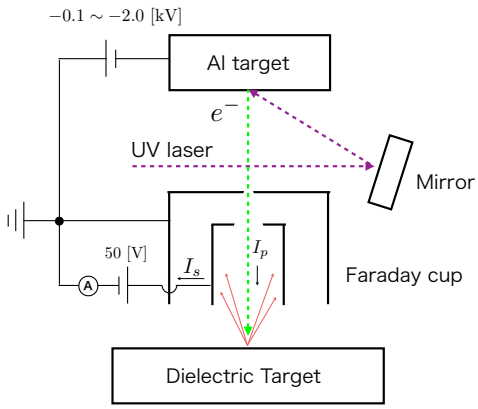

Figure 2: The overview of the experiment.

we can calculate the SEEC δ as

$$\delta = \frac{I_s}{I_p}. \tag{3}$$

Since the target is dielectric cells and does not conduct electricity, we cannot measure the primary current when we set the dielectric cells as a target. However, the primary current depends only on the laser power and bias applied on the aluminum target. Then we measure the primary electron using the aluminum plate as a target instead of the dielectric cells. Figure 3 shows the alternative target to measure the primary current I_p. The primary electron beam injects into the aluminum target and flows to the ground via the picoammeter.

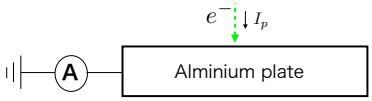

Figure 3: The alternative target to measure the primary current.

In the low E_p region, the terrestrial magnetism could be the dominant error of the beam spot if the flight length of the beam is too long or the beam energy is too small. Roughly, if $E_p = 0.1$ keV and the flight length is 40 mm, the error of the beam spot is $O(1)$ mm. In our setup, we made the flight length of the beam around 40 mm and consider the error of the beam spot as $\sigma \sim 1$ mm.

When measuring SEEC of the dielectric target, we need to consider the charging effect. If the SEEC is large $\delta > 1$, the beam spot becomes positively charged since the number of the emitted electrons are larger than one of the injected electrons. In this case, the electrostatic potential on the surface of the dielectric cell becomes positive, and the emitted electrons are attracted by the cell. Thus, after injecting many electrons to one spot, the SEEC becomes 1. Recently, the time-dependence of the secondary current $I_s(t)$ is understood as an equivalent circuital model in the literature [8] and the authors found the good agreement of their circular model and their results. Using the formulae driven

in Ref. [8], we can read off the SEEC δ by fitting the relaxation curve of the secondary current.

Figure 4 shows one of the dielectric cells used in the DAA structure. In order to accumulate the statistics of the measurement, we will measure one place until the secondary current becomes stable, then change the place to inject the beam by rotating the dielectric cells using the rotary motion-vacuum manipulator. We will rotate the cell by a fixed angle which corresponds to 2σ separation between each adjacent beam spot. Figure 5 shows the sectional view of the apparatus we manufactured for this measurement. In order to rotate the cell in the cylindrical chamber with a radius around 90 mm , the cell must be put on the holder connected with the rotary motion-vacuum manipulator in the bottom of the chamber and the electron beam must be shot from the top to the bottom.

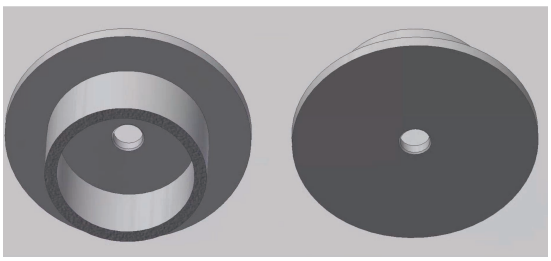

Figure 4: The dielectric cells used in the DAA structure seen from bottom of the cell (left) and top of the cell (right).

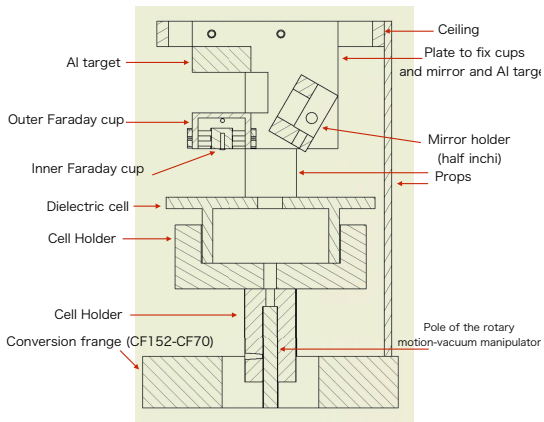

Figure 5: The sectional view of the apparatus that we designed to measure the SEEC of the dielectric cells.

Figure 5 shows the sectional view of the apparatus. All the three Aluminum parts are insulated by using the screw of alumina. The outer Faraday cup has a hole on the top of size ϕ 0.5 mm, while the inner Faraday cup has a hole on the top of size ϕ 3 mm. In order to shrink the flight length of the electrons, the cell holder becomes much high by tuning the coupling between the pole of the rotary motion-vacuum manipulator and the holders.

CONCLUSION

DAA structure is a candidate for the highly efficient accelerator which can realize continuous working at room temperature with a large current. Due to the large SEEC of the dielectric cells used in DAA structure, the multipactor followed by the breakdown is an obstacle to go to the high gradient region, $E_{\mathrm{acc}} >$ multi-MV/m. In order to overcome this problem, and realize the ultra-low loss accelerator with high gradient, it is indispensable to reduce the multipactor effect. In the DAA structure, the discharge effect around the beam axis due to the high SEEC may cause the multipactor effect, where the growing electron clouds eating the electrics. In order to manage both the reduction of the SEEC without spoil the benefit of the ultra-low loss dielectrics, we will try to locally apply TiN coating around the beam axis. We manufactured the apparatus to measure the SEEC of the dielectric cells both before and after the coating, to confirm that the uncoated cell energy region of $\delta(E_p) > 1$, and TiN coating decreases the δ.

After preparing all the setups e.g. enough power of the ultraviolet laser, we will start the measurement. First, we will measure the primary current I_p by introducing aluminum plate shown in Fig. 3 on the dielectric cell. We will clarify the table of the primary electron energy and its primary current. Then we remove the aluminum plate and measure the SEEC of the dielectric cells before and after the TiN coating. If we will confirm the reduction of the SEEC, we will again carry out the high voltage test and check whether the discharge effect is relaxed or not.

ACKNOWLEDGEMENTS

This work is supported by JSPS KAKENHI Grant No. 16H02134. The authors would like to thank N. Shigeoka from the Mitsubishi Heavy Industries Mechatronics Systems Ltd. for their continued support of the development of DAA structures. We would like to thank Makoto Ishizuka and Kawakami-san for their technical supports on the engineering and the vacuum setups.

REFERENCES

[1] D Satoh, M Yoshida, and N Hayashizaki. Dielectric assist accelerating structure. *Physical Review Accelerators and Beams*, 19(1):011302, 2016.

[2] D Satoh, M Yoshida, and N Hayashizaki. Fabrication and cold test of dielectric assist accelerating structure. *Physical Review Accelerators and Beams*, 20(9):091302, 2017.

[3] LB Mullett, W Walkinshaw, JS Bell, BG Loach *et al.* A theoretical and experimental investigation of anisotropic-dielectric-loaded linear electron accelerators. *Proceedings of the IEE-Part B: Radio and Electronic Engineering*, 104(15):273–290, 1957.

[4] J Rodney M Vaughan. Multipactor. *IEEE Transactions on electron devices*, 35(7):1172–1180, 1988.

[5] Peng Zhang, YY Lau, Matthew Franzi, and RM Gilgenbach. Multipactor susceptibility on a dielectric with a bias

dc electric field and a background gas. *Physics of Plasmas*, 18(5):053508, 2011.

[6] Asif Iqbal, John Verboncoeur, and Peng Zhang. Multipactor susceptibility on a dielectric with two carrier frequencies. *Physics of Plasmas*, 25(4):043501, 2018.

[7] J Rodney M Vaughan. A new formula for secondary emission yield. *IEEE Transactions on Electron Devices*, 36(9):1963–1967, 1989.

[8] David Bañón-Caballero, Juan M Socuéllamos, Rafael Mata, Laura Mercadé, Benito Gimeno, Vicente E Boria, David Raboso, Vladimir E Semenov, Elena I Rakova, Juan F Sánchez-Royo *et al*. Study of the secondary electron yield in dielectrics using equivalent circuital models. *IEEE Transactions on Plasma Science*, 2018.